

A Cartesian Robot for RFID Signal Distribution Model Verification

Aliasgar Kutiyawala and Vladimir Kulyukin

Computer Science Assistive Technology Laboratory (CSATL)
Department of Computer Science
Utah State University
Logan, UT, 84322
aliasgar@cc.usu.edu, vladimir.kulyukin@usu.edu

Abstract. In our previous research, we addressed the problem of automating the design of passive radio-frequency (PRF) services. An optimal PRF surface is one that offers a maximum probability of localization at a minimum instrumentation cost, i.e., a minimum number of surface-embedded passive RFID transponders. Our previous results were based on the assumption that the signal distribution model of an individual RFID transponder can be approximated as a circle. The problem of automated PRF surface design was then formulated as the problem of packing a surface with circles of a given radius. However, in practice, this approach leads to some loss of optimality: some areas of the surface may not be covered or too many transponders may be required. More exact methods are needed for verifying and constructing signal distribution models of surface-embedded RFID transponders that can be used by surface packing algorithms to optimize the design. In this paper, we present the design and implementation of a Cartesian robot for verifying and constructing signal distribution models of surface-embedded RFID transponders. A model is characterized by four high-level parameters: an RFID transponder, an RFID antenna, an RFID reader, and a surface type. The robot moves an RFID reader-antenna unit over a PRF surface, e.g. a carpet, and systematically collects readings for various antenna positions over the surface. The collected readings are subsequently processed to verify or construct signal distribution models. We describe experiments with the robot to verify the localization probability of automatically designed PRF surfaces. We also present experiments with the robot to verify and construct the signal distribution models of a specific RFID transponder.

1 Introduction

A smart environment is a regular everyday environment instrumented with embedded sensors and computer systems that make use of the data they receive from those sensors to support a quality-of-life function [1]. Since many smart environments are composed of surfaces, one can pose the question of how PRF sensors can be embedded into those surfaces to improve the functionality of mobile units operating in those environments. In our previous research [11, 12], we addressed the problem of automating the design of PRF services. An optimal PRF surface is one that offers a maximum localization probability at a minimum cost, i.e., a minimum number of embedded RFID transponders. The cost of the surface material is presently not taken into account. Our previous results were based on the explicit assumption that the signal distribution model of an individual RFID transponder can be approximated as a circle. The problem of automated PRF surface design was then formulated as the problem of packing a surface with circles. However, in practice, this approach leads to some loss of optimality: some areas of the surface may not be covered or too many transponders may be required.

More exact methods are needed for verifying and constructing the signal distribution models of surface-embedded RFID transponders that can be used by surface packing algorithms to optimize the design. In this paper, we present the design and implementation of a Cartesian robot for verifying and constructing signal distribution models of surface-embedded RFID transponders. A model is characterized by four high-level parameters: an RFID transponder, an RFID antenna, an RFID reader, and a surface type. The robot moves an RFID reader-antenna unit over a PRF surface, e.g. a carpet, and systematically collects readings for various antenna positions over the surface. The collected readings are subsequently processed to verify or construct signal distribution models.

Several research efforts are related to our research. Patterson et al. [6] use glove-embedded RFID readers that detect RFID stickers on various household objects to monitor the activities of seniors in their homes. Willis and Helal [7] propose an assisted navigation system where an RFID reader is embedded into a blind navigator's shoe and passive RFID sensors are placed in the floor. Kantor and Singh use RFID tags for robot localization and mapping [8]. Once the positions of the RFID transponders are known, their system uses time-of-arrival type of information to estimate the distance from detected tags. Tsukiyama [10] developed a navigation system for mobile robots using RFID transponders under the assumption of perfect signal reception and zero uncertainty. Hähnel et al. [9] developed a probabilistic robotic mapping and localization system to analyze whether RFID can be used to improve the localization of mobile robots in office environments.

2 Reading a RFID Transponder

Figure 1 shows a typical setup of a passive RFID system. The RFID reader takes in a command (usually in the form of a string) from the user, generates the required signals and transmits them in the form of electromagnetic waves through the antenna. This electromagnetic signal excites a small coil in the RFID transponder and charges a capacitor inside the transponder. The energy stored inside the capacitor powers up a circuitry inside the transponder and a unique ID is transmitted back through the coil. The antenna receives this unique ID in the form of an electromagnetic signal decoded by the RFID reader. The reader sends this unique ID back to the user in the form of a string.

For the antenna to read the transponder, enough electromagnetic voltage must be induced in the transponder's coil to charge up the capacitor. The amount of electromagnetic voltage induced in the coil depends upon the transponder's position with respect to the antenna (in terms of x, y, z coordinates), the transponder's orientation with respect to the antenna (θ), the dielectric constant (k) of the material between the antenna and the transponder, the type of antenna and transponder, and the power (V) given to the RFID reader.

If we assume that the dielectric constant and power given to the RFID antenna are constant, we can develop a function $f(x, y, z, \theta) = \{true, false\}$ for a given antenna-transponder unit. This function describes whether a given transponder placed at the coordinates (x, y, z) and at an orientation θ with respect to the antenna, can be read by the antenna or not. An *isofield* or a *charge-up* diagram provides a visual description of such a function. Figures 2(a) through 2(b) show the isofield diagrams for the Series 2000 stick antenna from Texas Instruments and are obtained from the Texas Instruments Antenna Reference Guide [14].

The read area of a RFID transponder is defined as the area where the antenna can read the transponder. The read areas of a transponder can be visualized in Figures 9(a) through 9(d). The read area of a transponder can be defined as $R = \{(x, y, z, \theta) | f(x, y, z, \theta) = true\}$. In our previous research [11], we proposed several algorithms for designing PRF surfaces on the assumption that the read area is a circle of radius r . However, the actual read area has a butterfly-like shape.



Fig. 1. Typical RFID Setup.

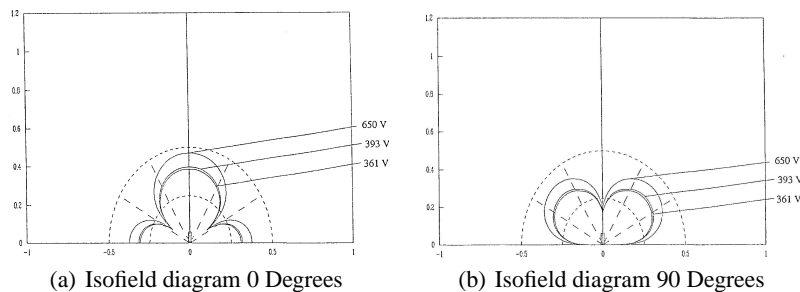


Fig. 2. Isofield diagrams for the stick antenna (a) Orientation of tag = 0 degrees (b) Orientation of tag = 90 degrees.

3 Optimality of PRF Surfaces

A PRF surface is defined as a surface embedded with passive RFID tags. A mobile unit, such as a walker for the elderly, that operates in a smart environments can utilize either *proprioception* (action is determined relative to an internal frame of reference) or *exteroception* (action is determined from a stimulus originating in the environment itself). The primary purpose of a PRF surface is to make it possible for a mobile device, e.g. a walker for the elderly [13], to perform exteroceptive localization reliably. In order to localize, the device must be able to read at least one of the transponders embedded in the PRF surface. Once a transponder is read, the unit immediately localize by retrieving the transponder’s position from a previously compiled database that maps transponder IDs to positions.

We define *localization probability* as the probability of the mobile device reading at least one transponder as its crosses the surface from one side to another on a straight line. One way to increase the localization probability is to populate the surface with more transponders. While this method is guaranteed to increase the localization probability, it will also increase the cost of the surface. To address this trade-off, we define the *optimality* of a PRF surface as the ratio of the localization probability to the cost, i.e. the number of surface-embedded transponders. Thus, to increase the optimality, the localization probability must be increased without a proportionate increase in the number of transponders embedded in the PRF surface.

Optimality can be increased by placing the transponders at strategic locations on the surface. We used this idea to develop four algorithms for automatically designing optimal PRF surfaces. To make the presentation more complete, we present only a brief description of each algorithm below. An interested reader is referred to [11].

- **Brute-Force Method:** All possible placement patterns are computed for a given PRF surface. The localization probability is computed for each pattern. The pattern with the highest localization probability is chosen as the final design.
- **Static Greed:** RFID transponders are placed at intersection points of the different paths taken by a mobile unit to cross the PRF surface. The weight of each intersection is computed to be the number of paths passing through it. The first transponder is placed at the intersection point with the highest weight, the second transponder is placed at the next available intersection point with the second highest weight and so on.
- **Dynamic Greed:** RFID transponders are placed at intersection points of the different paths taken to cross the surface. The weight of each intersection is computed as the number of paths passing through it. The first transponder is placed at the intersection point with the highest weight. Paths passing through this intersection point are excluded from subsequent transponder placements and the weights are recomputed. The next transponder is placed at the intersection point with the highest weight and so on.
- **Hill-Climbing:** Transponders are initially placed at random positions. A responder is randomly chosen, and is moved by a random amount in a random direction. The localization probability is calculated at this position. If this localization probability is greater than the previous localization probability, the move is accepted, otherwise the move is rejected. This process is continued until the localization probability does not change over several consecutive iterations.

Of the four algorithms described above, only the brute force method guarantees an optimal PRF surface design. However, it runs in exponential time and is not practical for large PRF surfaces. The other algorithms produce designs that are reasonably optimal and run in polynomial time. All algorithms repeatedly compute the localization probability. Figure 3 shows a PRF surface embedded with one transponder. Suppose there is a mobile unit equipped with one RFID antenna crossing the PRF surface from side A to side B. Since the width of the surface is assumed to be small, we assume that the unit will travel only along a straight line (path). To reduce the computational complexity, let us discretize each side (A and B) into n points and further assume that the unit will cross the surface only along one of the lines connecting the n points A to the n points on B. The read area of the transponder is assumed to be a circle having the transponder as its center. The unit can read the transponder if it crosses the surface along one of the paths that intersect the circle (shown by light gray colored lines) and cannot read the transponder if the path does not intersect the circle (shown by dark gray colored lines). The localization probability is computed as $p = \frac{n_r}{n_t}$, where n_r is the number of paths that cross the circle and n_t is the total number of paths.

For the surface in Figure 3, the localization probability is 62%. The optimality of the surface is computed as $\frac{p}{n_{tags}}$. In this case, we say that the optimality of the surface is also 62% since $n_{tags} = 1$.

4 A Cartesian Robot

To visualize the read area of a transponder, we performed a simple experiment: we placed a transponder on a surface and then placed an antenna at various points around it to check if the transponder could be read. This experiment, though tedious and

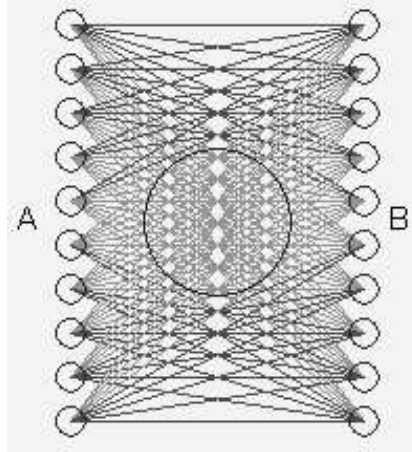


Fig. 3. Probability of localization of a PRF surface.

error prone, gave us a rough estimate of the read area. It also provided us with an idea to design a robot that would automate the entire process. The requirements of this robot were to scan a RFID transponder automatically and provide the read area as the final output.

We found a range of ± 25 cms along the X and Y axes to be sufficient for transponder scanning. We allowed the antenna's height to range from 2.5cms to 10cms so that the read areas could be obtained at different heights of the antenna with respect to the transponder. The granularity of the scan depended upon the resolution at which the transponder was scanned. We found that a minimum resolution of 2mm was necessary to produce a sufficiently detailed image of the read area. We minimized the use of ferromagnetic materials in the robot to reduce the ferromagnetic interference..

The last requirement did not allow us to buy off-the-shelf Cartesian robots as most of them are made using metals. We decided to design our own Cartesian robot that would satisfy the requirements. Figure 4 shows the robot's design and Figure 5 shows the actual robot. Its design uses two linear actuators (part number: E57H42-2.7-007ENG from Haydon Switch and Instruments) having a range of 60cms. The actuators are placed perpendicular to each other to ensure scanning along the X and Y axes, respectively. An earlier design had one linear actuator being driven by another linear actuator so that the PRF surface would be on the ground and the antenna would move in a raster pattern. Since the two linear actuators were connected to each other, there were issues with balancing the entire system due to uneven weight distribution. This design had to be abandoned in favor of the current design that disconnects the actuators from each other. In the current design, one linear actuator drives a table-top (on which the PRF surface rests) along the X axis while the other actuator drives the antenna along the Y axis. Thus, the antenna can scan the surface along a raster pattern. The table-top rests on two sliders that restrict its movement along the X axis. The antenna is placed on a wooden block and two wooden guides restrict the movement of this block to the X axis. Since most of the construction is done with wood, the ferromagnetic interference is minimal.

The electronic subsystem is as shown in Figure 6. The linear actuators are connected to their respective stepper motor drivers (part number: DCM 8028 from Haydon Switch and Instruments). These drivers move the stepper motors in the actuators by receiving pulses from an OOPIC microcontroller that is connected to the PC/Laptop via a USB to Serial converter. The amount of movement, and hence the resolution of the scan, is controlled by the number of pulses given to the stepper motor driver. The RFID antenna (Series 2000 stick antenna from Texas Instruments) is connected to a RFID reader (Series 2000 Standard Reader from Texas Instruments) connected to the PC/Laptop via another USB-Serial Converter. A Java program runs on the PC/Laptop and communicates with the OOPIC microcontroller and RFID reader to scan the PRF surface.

To scan the PRF surface, the PRF surface is placed on the table-top and the actuators are reset to their default positions. The antenna is then moved along the Y axis by a small amount (equal to the resolution of the scan). A transponder on the PRF surface is read n times. The boundary of the read area is fuzzy and usually the reader reads the transponder only m times, where $m \leq n$ instead of n times. This helps us identify the fuzziness of the boundary of the read area as a percentage of times the transponder can be read at that place. While performing the experiments, we chose a value of $n = 3$. A higher value of n will help in identifying the fuzziness of the boundary with a higher resolution but it will also take more time to

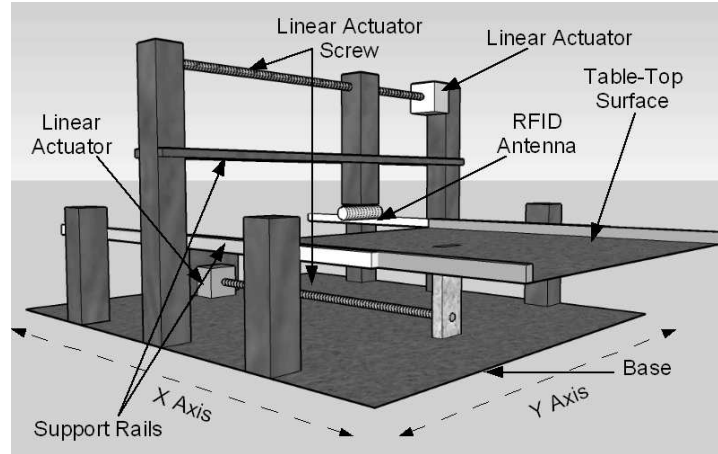


Fig. 4. Model of the Cartesian Robot.



Fig. 5. The Cartesian Robot.

scan. The value of m and the corresponding position (x, y) are saved in the database. The antenna is moved again along the Y axis and the transponder is read again.

This procedure is repeated until the antenna is at a distance of 50cms from the starting position. Now the table-top is moved by a small distance (again equal to the resolution of the scan) and the PRF surface is scanned again by moving the antenna backwards along the Y direction and attempting to read the tag. The antenna is moved backwards until it returns to its original location. The table-top is once more moved along the X axis and the PRF surface is scanned along the Y axis. This procedure is repeated till the table-top is at a distance of 50cms from the original location. This procedure ensures that the PRF surface is scanned uniformly along both the dimensions. The range and resolution of movement along either axis can be controlled independently from the computer.

5 Experiments with the Cartesian Robot

5.1 Verifying Localization Probabilities of PRF Surfaces

Each of the four algorithms used to design PRF surfaces produces the localization probability of the PRF surface. The localization probabilities are computed assuming that the read area of the transponder is a circle centered on the transponder. In our

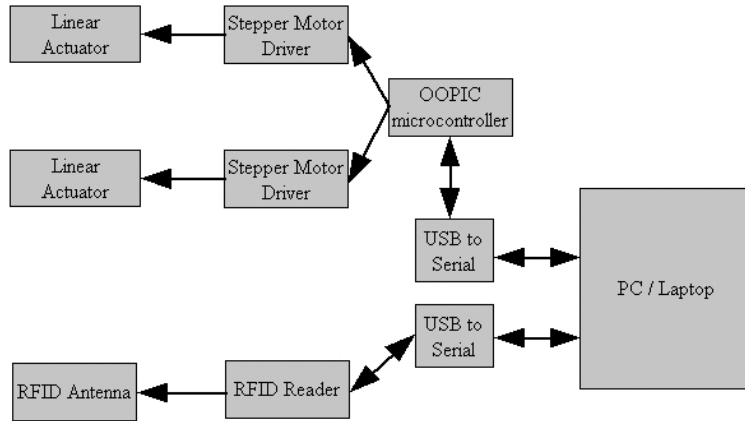


Fig. 6. Electronic Subsystem of the Cartesian Robot.

first experiment, we wanted to investigate how well the localization probabilities computed by the algorithms approximate the actual localization probabilities.

We designed a PRF surface using each of the four algorithms mentioned and noted down the algorithmic localization probability for each PRF surface. Then we built the PRF surfaces using the placement pattern computed by the algorithm and placed the surface on the table-top of the Cartesian robot. The robot was then made to scan the surface. For each position (x, y) of the antenna with respect to the transponder, it was noted if the antenna could read the tag or not. Finally, the robot's output was analyzed to produce the actual localization probability.

All four algorithms were provided with the same inputs for designing the surface: width = 30cms; length = 60cms; number of transponders = 2. Table 5.1 shows the positions of the transponders on the PRF surface and compares the algorithmic and actual localization probabilities for the four surfaces.

Table 1. Verification of Probability of Localization using the Cartesian Robot.

	Tag 1	Tag 2	Theoretical Probability	Actual Probability
Brute Force Method	(15, 11)	(15, 29)	87.77%	88.72%
Static Greed	(15, 18)	(15, 40)	79.22%	81.22%
Dynamic Greed	(15, 11)	(15, 29)	79.22%	81.22%
Hill Climbing Method	(16, 19)	(15, 40)	87.77%	89.33%

The designs generated by both Greedy methods are the same and the designs generated by the Brute Force method and the Hill Climbing method are very similar. The Brute Force and Hill Climbing methods provided better designs than the Greedy methods and this can be observed from their localization probabilities. The last two columns of the table show that the actual probabilities of localization compare well to the algorithmic ones. The results of a t-test for this sample shows that the differences between the algorithmic and actual probabilities are statistically insignificant. The slight differences can be attributed to the coarseness of the data sample and discretization errors in calculating the actual probabilities and approximating the read area as a circle in the algorithms.

5.2 A Signal Distribution Model of an RFID Transponder

We also conducted experiments with the robot to verify the isofield diagrams from Texas Instruments and to construct a mathematical signal distribution model of the transponder. The procedure for performing both experiments was as follows. The transponder was placed on the table-top of the Cartesian robot such that it was at an angle of zero degrees with respect

to the antenna, and a scan was performed. The transponder was then rotated in increments of 90 degrees (until it was back to its original orientation of zero degrees with respect to the antenna), and a scan was performed after each increment. This procedure ensured that we had the read area of the transponder for all orientations with respect to the antenna. This experiment was repeated for different heights (1.5 inches and 2 inches) of the antenna with respect to the transponder.

The verification of the isofield diagrams was performed visually by comparing the pictures of the transponder's read area obtained by the experiment and the ones provided by Texas Instruments in their manual. This procedure did not require high resolution scans of the transponder. Therefore, the robot took readings every 10mm along the X and Y axes. Figures 9(a) through 10(d) show the output (read areas of the transponder) of the eight scans (four scans for a given height). The transponder is denoted by a small square shaped dot. The read area is represented by rings of various shades of gray. A black ring means that the transponder was read in every time whereas a light gray ring means that the tag was read only in some times. The light gray colored rings are usually present at the boundary of the read area and imply that the boundary of the read area is fuzzy.

The isofield diagrams obtained from Texas Instruments are inverted and appended to themselves and are shown in Figures 11(a) and 11(b). Figures show that our results are reasonably similar to the ones from Texas Instruments. Thus, the robot was able to verify their isofield diagrams. By looking at the read areas we can also see that they are symmetric and that the read areas for orientations differing by 180 degrees are similar. We can observe that the read area decreases in size as the height of the antenna with respect to the transponder increases.

The transponder had to be scanned with a much finer resolution to obtain a mathematical model. Specifically, the robot took readings in increments of 2mm along both axes. This increased the number of readings by a factor of 25. Readings were taken at all four orientations and for various antenna heights with respect to the transponder. The readings were imported into MATLAB and segmented into four quadrants as shown in Figure 7. A mathematical model was developed for each quadrant. Since each quadrant looks like an oval, it was observed that developing a mathematical model in polar coordinates would be easier. The center of the quadrant was found by finding the center of mass for the quadrant. If the transponder could be read at a point, a mass of one was assigned to that point otherwise a mass of zero was assigned. Once the center of the quadrant was found, the distance (r_ϕ) of the farthest point having a mass of one along an angle ϕ was calculated and this pair (r_ϕ, ϕ) was saved. Now a function ($f(\phi) = r_\phi$) was calculated by using the MATLAB function `polyfit`. Curve fitting was performed for different degrees of the resulting polynomial and the error between the curve-fitted polynomial model and the actual data was calculated using the MATLAB function `polyval`. Polynomial models having the least error were chosen as the final mathematical model.

The following equations describe the mathematical model for each of the four quadrants:

- Mathematical model for the first quadrant: $f(\phi) = -0.0006\phi^3 + 0.0167\phi^2 - 0.1915\phi + 15.460$
- Mathematical model for the second quadrant: $f(\phi) = 0.0001\phi^3 - 0.0018\phi^2 - 0.0051\phi + 16.7399$
- Mathematical model for the third quadrant: $f(\phi) = -0.0004\phi^3 + 0.0142\phi^2 - 0.0953\phi + 17.2427$
- Mathematical model for the fourth quadrant: $f(\phi) = -0.0006\phi^3 + 0.0151\phi^2 - 0.2012\phi + 16.1954$

Figures 8(a) through 8(d) show the plots of the derived mathematical model and the actual data. It can be observed that the resulting error between the two is very low and that the derived polynomials are adequate models for this type of RFID transponder.

These four polynomials can be integrated into one model by choosing the appropriate model at run time. One of the quadrants would be selected depending on the position of the antenna and the distance (d) and the angle (ϕ) of the antenna with respect to the center of the quadrant would be computed. The corresponding polynomial would give the distance $r_\phi = f(\phi)$ for the angle ϕ . If $d \leq r_\phi$, it is determined that the antenna lies in the read area and can read the transponder.

6 Future Work

We intend to further refine the development of mathematical models of RFID transponders. One approach is to analyze the electromagnetic interaction between the antenna and the transponder. We can model the coils of the antenna and the transponders using well developed antenna models (monopole, dipole, etc) and analyze the electromagnetic signal distribution between them. Once we develop the parameterized model of the electromagnetic signal distribution, we can obtain the parameters of the model by performing more experiments with our robot.

Another approach is to perform very fine resolution scans of the read area of the transponder using the Cartesian robot and develop a "black box" model of the transponder by curve fitting the data. This kind of model would be in polar coordinates

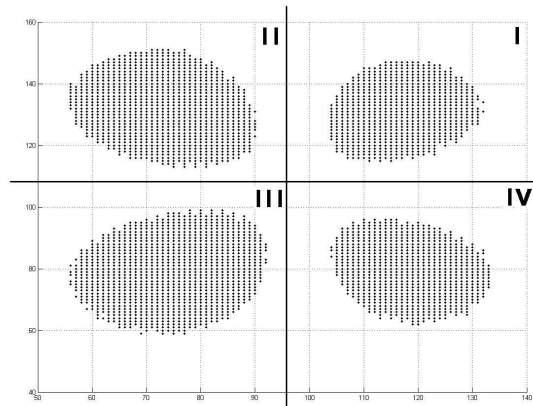


Fig. 7. Dividing the read area into four quadrants.

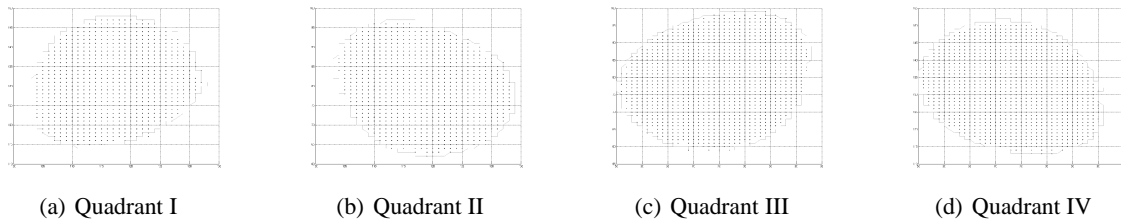


Fig. 8. Models for (a) Quadrant I (b) Quadrant II (c) Quadrant III (d) Quadrant IV.

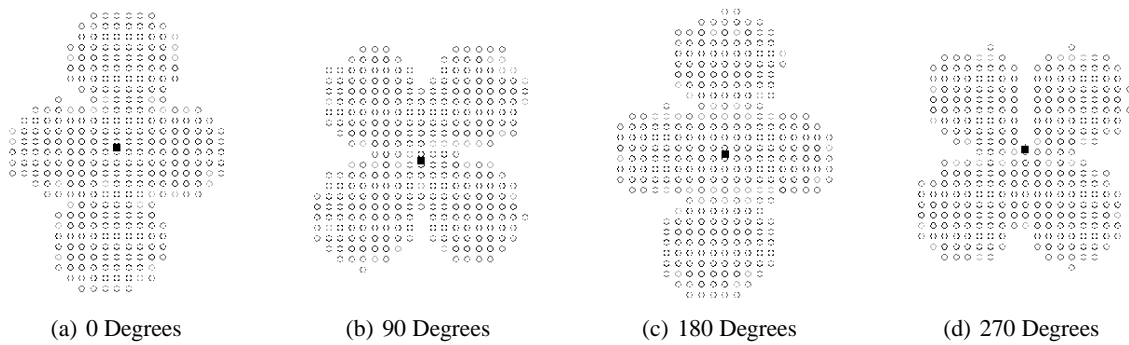


Fig. 9. Antenna Height = 1.5 inches (a) 0 Degrees (b) 90 Degrees (c) 270 Degrees (d) 180 Degrees.

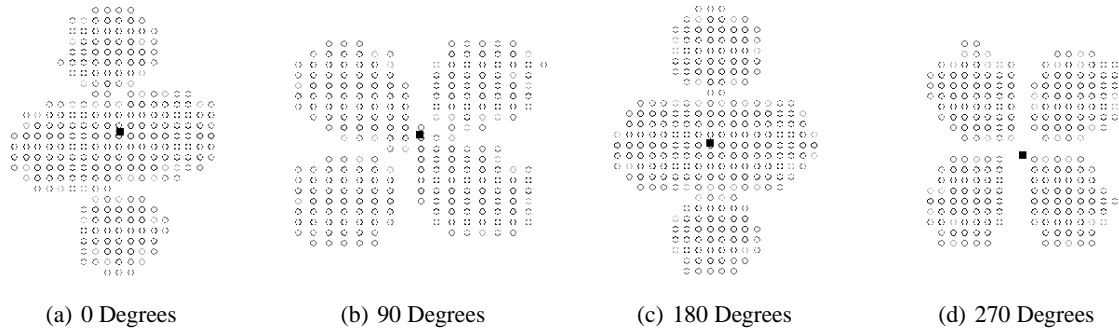


Fig. 10. Antenna Height = 2 inches (a) 0 Degrees (b) 90 Degrees (c) 270 Degrees (d) 180 Degrees.

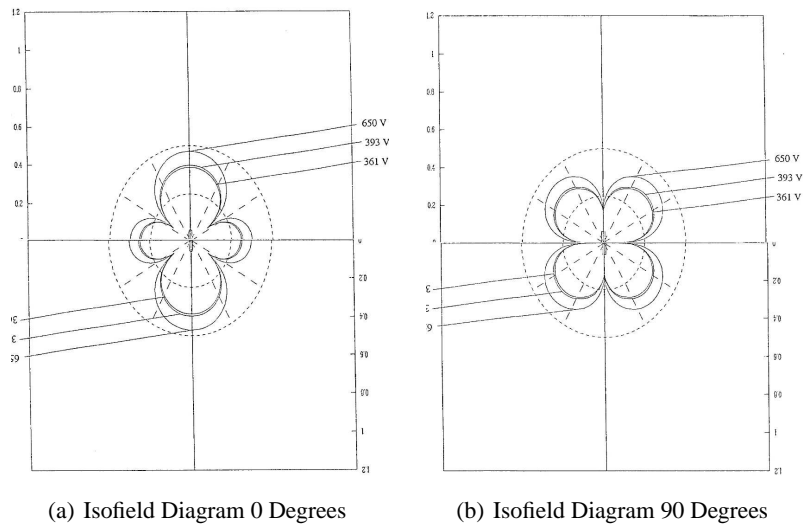


Fig. 11. (a) Isofield Diagram 0 Degrees (b) Isofield Diagram 90 Degrees.

centered on the transponder and will provide the maximum distance at which the transponder could be read along a particular angle. We would prefer to develop a three-dimensional model that also incorporates the height of the antenna with respect to the tag. If such a model is not possible, we would develop different two-dimensional models for different heights of the antenna with respect to the transponder.

7 Conclusion

Optimally designed PRF surfaces can help reduce the cost of indoor localization. We have presented a Cartesian robot that can verify the optimality of PRF surface designs by computing the actual probability of localization on that surface. The robot can also be used to verify and develop signal distribution models of RFID transponders that can be used in designing more optimal PRF surfaces.

We performed experiments to verify the optimality of PRF surface design by showing that the error between the actual and algorithmic localization probabilities is statistically insignificant. We also performed experiments to model the read area of a RFID transponder for different orientations and heights of the antenna. Using these read areas we verified the read area of the RFID transponder reported by Texas Instruments. We also developed a mathematical model of the transponder and shown that the error between the mathematical model and actual data is very low.

8 Acknowledgments

The second author would like to acknowledge that this research has been supported, in part, through NSF CAREER grant (IIS-0346880) and three Community University Research Initiative (CURI) grants (CURI-04, CURI-05, and CURI-06) from the State of Utah.

References

1. Zita Haigh, K. and Kiff, L.M. and Myers, J. and Guralnik, V. and Gieb, C. and Phelps, J. and Wagner, T. *The Independent Life Style Assistant: AI Lessons Learned* Proceedings of the 2004 IAAI Conference, 2004
2. Pollack, M. *Intelligent Technology for the Aging Population* AI Magazine, 2005
3. Kautz, H. and Arnstein, L. and Borriello, G. and Etzioni, O. and Fox, D. *An Overview of the Assisted Cognition Project* Proceedings of the 2002 AAAI Workshop on Automation as Caregiver: The Role of Intelligent Technology in Elder Care, 2002
4. Marston, J. and Golledge, R. *Towards an Accessible City: Removing Functional Barriers for the Blind and Visually Impaired: A Case for Auditory Signs* Technical Report, Department of Geography, University of California at Santa Barbara, 2000
5. AMS Project *Autonomous Movement Support Project* <http://www.ubin.jp/press/pdf/TEP040915-milt01e.pdf>
6. Patterson, D. and Fishkin, K. and Fox, D. and Kautz, H. and Perkowitz, M. and Philipose, H. *Contextual Support for Human Activity* Proceedings of the 2004 AAAI Spring Symposium on Interaction between Humans and Autonomous Systems OverExtended Operation, 2004
7. Willis, S. and Helal, S. *A Passive RFID Information Grid for Location and Proximity Sensing for the Blind User* University of Florida Technical Report number TR04-009, 2004
8. Kantor, G. and Singh, S. *Preliminary Results in Range-Only Localization and Mapping* IEEE Conference on Robotics and Automation, 2002
9. Hahnel, D. and Burgard, W. and Fox, D. and Fishkin, K. and Philipose, M. *Mapping and Localization with RFID Technology* Technical Report, IRS-TR-03-014, Intel Research Institute, 2003
10. Tsukiyama, T. *Navigation System for Mobile Robots using RFID tags* IEEE Conference on Advanced Robotics, 2003
11. Kulyukin V. and Kutiyawala A. and Jiang M. *Surface-embedded Passive RF Exteroception: Kepler, Greed, and Buffon's Needle* Proceedings of the Fourth International Conference on Ubiquitous Intelligence and Computing (UIC 2007), Hong Kong, China, July 2007.
12. Minghui, J. and Kulyukin, V. *Connect-the-Dots in a Graph and Buffon's Needle on a Chessboard: Two Problems in Assisted Navigation*. Proceedings of the 10th Joint Conference on Information Sciences and the 10th International Conference on Computer Science and Informatics (JCIS-CSI-07). Salt Lake City, UT, July, 2007.
13. Kulyukin V. and LoPresti E. and Kutiyawala A, and Simpson R. and Matthews J. *A Rollator-Mounted Wayfinding System for the Elderly: Proof-of-Concept Design and Preliminary Technical Evaluation* Proceedings of the 30-th Annual Conference of the Rehabilitation Engineering and Assistive Technology Society of North America (RESNA 2007), 2007
14. Texas Instruments *Antenna Reference Guide* <http://focus.ti.com/lit/ug/scbu025/scbu025.pdf>, 1999